ORIGINAL ARTICLE

Performance of the Nanobio-Based Reagent for Visualising Wet Fingerprints Exposed to Different Levels of Water Salinity

Chao Wen Ting[1], Naji Arafat Mahat[1,2,3,4], Aida Rasyidah Azman[1,2], Nor Wajihan Muda[1,2], Nurazira Anuar[1]

1 Department of Chemistry, Faculty of Science, Universiti Teknologi Malaysia, Johor, Malaysia
2 Enzyme Technology and Green Synthesis Research Group, Faculty of Science, Universiti Teknologi Malaysia, Johor, Malaysia
3 Centre for Sustainable Nanomaterials, Ibnu Sina Institute for Scientific and Industrial Research, Universiti Teknologi Malaysia, Johor, Malaysia
4 Centre of Research for Fiqh Forensics and Judiciary, Universiti Sains Islam Malaysia, Negeri Sembilan, Malaysia

Corresponding authors:
Naji Arafat Mahat and Aida Rasyidah Azman,
Department of Chemistry,
Faculty of Science,
Universiti Teknologi Malaysia,
81310 Skudai,
Johor, Malaysia.
Email: naji.arafat@utm.my;
        aidarasyidah@rocketmail.com

ABSTRACT

Introduction: Recovery of evidence such as murder weapons in waterways has been commonly reported. However, visualising latent fingerprints on the immersed substrates may prove challenging due to its obliteration by physicochemical parameters (e.g. pH, temperature, salinity) as well as the mechanical effect of water. Although the use of Small Particle Reagent (SPR) for visualising latent fingerprints on wet non-porous substrates has been suggested, it contains molybdenum and titanium that are toxic, and their utilisation must be reduced. Furthermore, no study verifies the chemical and/or physical interaction between SPR and the lipid constituents of wet latent fingerprints that leads to the visualisation of ridge details. **Methods:** The SPR and newly developed nanobio based reagent (NBR) i.e. *Candida rugosa* lipase-multiwalled carbon nanotubes (CRL-MWCNTs) were used for visualising latent fingerprints on glass slides immersed in water with salinity levels representing those of estuary and swimming pool for up to 15 days. **Results:** It was observed that the quality of the visualised fingerprints using NBR was comparable with that of SPR. Characterisations *via* instrument and bioinformatics analyses have also verified the incorporation of CRL onto MWCNTs and the chemical interaction between NBR and lipid constituents of wet latent fingerprints. **Conclusions:** Therefore, the newly developed NBR may prove a promising relatively greener alternative for substituting SPR for visualising latent fingerprints on glass slides immersed in different levels of water salinity.

KEYWORDS: Nanobio-based reagent, *Candida rugosa* lipase, wet latent fingerprints, saline water, forensic science

INTRODUCTION

Fingerprint is one of the most reliable current gold standards of biometric features for human identification [1], particularly involving forensic criminal investigations. This physical evidence has a unique combination of characteristics that ties it to an individual, object and/or location. The admissibility of fingerprint evidence in the court of law relies on the fact that it is (1) unique to only an individual, (2) permanent throughout an individual's lifetime and can be (3) systematically classified into general ridge patterns. The fingerprints found at the scenes of crime can exist in the form of patent, plastic, and/or the more common

ones: latent. Because latent prints require appropriate visualisation methods due to their hidden nature, the selection of such method is contingent on the nature of the substrates (e.g. porosity and wetness/dryness) [2], among many other factors.

More often than not, criminals tend to discard/conceal any evidence of wrongdoing (e.g. weapons) in destructive environmental conditions such as waterways [3]. Considering that fingerprints are primarily made up of water-soluble constituents (e.g. proteins and amino acids) from the eccrine glands, the water itself may washed off such constituents, leaving only the non-water-soluble constituents (e.g. fatty acids and wax) secreted by the sebaceous glands.

32

Furthermore, the depredation of water-immersed evidence by aquatic fauna (e.g. fishes and snails) may tamper, or otherwise destroy, the fingerprints. The fact that recovering such prints on wet evidence is forensically challenging, the physicochemical parameters of water (e.g. pH, turbidity, and salinity) itself might further accelerate the rate of fingerprint deterioration on such substrates. While investigating the recovery of fingerprints immersed in fresh and sea waters, Madkour et al. [4] found out that the fingerprints had deteriorated at a much faster rate in high salinity water when compared to the ones immersed in fresh water.

Although there are a number of available lipid reagents for visualising such prints (e.g. Oil Red O and Sudan black), Small Particle Reagent (SPR) has been the typical reagent used by police officers and forensic scientists worldwide. Conventionally, SPR is a suspension of fine particles of molybdenum disulphide (MoS_2) or titanium dioxide (TiO_2) in a surfactant, globally monopolised by an American-based company Sirchie. Presumably targeting lipid-soluble constituents of fingerprints, SPR has been routinely used for on-site as well as laboratory visualisation of latent fingerprints on wet, non-porous substrates [5,6]. Because the use of SPR requires rinsing, possibly multiple of times, toxic metal build-ups like those of MoS_2 and TiO_2 in the drainage system may pose an unwanted, critical hazardous impact to the ecosystem, for both short- and long-terms use. For instance, the International Agency for Research on Cancer has reported that TiO_2 would induce carcinogenesis in animals, and possibly humans too [7]. Taking into account the imperative need to visualise such prints for forensic purposes as well as the potential hazard SPR poses, development of a relatively greener reagent is therefore deemed necessary.

Review of literature revealed the specific use of a relatively greener wet fingerprint visualisation method utilising lipases (from *Candida rugosa*) as the biosensor for lipid detection [8-11]. Although such studies reported the successful developments of green lipase-based reagent, the studies however were tailored for visualisation of fingerprints on non-porous substrates immersed in fresh waters (i.e. tap and lake). Considering that salt water makes up most of the Earth water distribution (about ~ 97.5%) [12], investigation

into the feasibility of such reagent in visualising latent fingerprints immersed in a much destructive aquatic environment may prove forensically significant.

Since the nanobio-based reagent (NBR) developed by Azman et al. [10] offers rapid fingerprint visualisation (about 2 mins) with a single application, the reagent was chosen for comparing with the standard SPR. Hence, this study is aimed at investigating the performance of NBR for visualising latent fingerprints on non-porous substrate (i.e. glass slides) immersed in different levels of water salinity (estuary- and swimming pool-like) for up to 15 days under laboratory-controlled settings. Additionally, this study provides characterisation of the NBR (*via* Attenuated Total Reflectance – Fourier Transform Infrared Spectrometry, ATR-FTIR and Field Emission Scanning Electron Microscopy, FESEM) as well as *in silico* insights of the specific attachment of the NBR with selected fatty acids found in wet fingerprints (*via* molecular docking and molecular dynamics simulations).

MATERIALS AND METHODS

Materials

While the *C. rugosa* lipase (CRL) (Type VII; ≥ 700 unit/mg solid) and acid-functionalised multiwalled carbon nanotubes (F-MWCNTs) were both procured from Sigma-Aldrich (St. Louis, USA) and Usains Holdings Sdn. Bhd. (Universiti Sains Malaysia, Malaysia), respectively, the SPR was obtained from Sirchie (Youngsville, USA). Acetone (99% purity) and potassium phosphate buffer (pH 7) were bought from QRëC (Selangor, Malaysia). The sodium chloride crystals were bought from Merck (Germany).

Preparation of the NBR

About 100 mg of partly purified CRL in 25 mL of phosphate buffer (pH 7) was centrifuged at 60 rpm for about 5 mins. The supernatant was then used for the immobilisation of CRL onto 75 mg of F-MWCNTs, magnetically stirred for 5 hr at 4 °C. For removing the unbound CRL, the solution was washed repeatedly with the same phosphate buffer (about 3 times). Afterwards, the solution (NBR) was stored in an opaque plastic bottle at 4 °C until further use [10].

Experimental Design

While the characterisation of NBR using ATR-FTIR (Frontier, Perkin Elmer) was done for confirming the successful immobilisation of CRL onto the F-MWCNTs, FESEM (SU8020, Hitachi), bioinformatics analyses (*viz.* molecular docking and dynamics simulations) (GROMACS version 2018.6) were employed for providing the computational support for the successful attachments of NBR onto the lipid-lined ridges of fingerprints, respectively.

Groomed split fingerprints from the right thumbs of four donors from both males and females (two from each gender aged between 20 – 40 years old) were deposited on acetone-cleaned glass slides in triplicates. For obtaining such prints, the donors were asked to gently rub their thumbs against their T-zones and further deposited the fingerprints at the joint of two identical glass slides for approximately 3 s (contact time), thereby splitting the groomed fingerprints into two equal halves. For each fingerprint deposition process, an allowable gap of 5 mins was practiced. The glass slides bearing fingerprints were then individually secured onto a cylinder-like plastic mesh with nylon cable ties prior to immersion in two separate PVC containers filled with tap water of different salinity levels: (1) 800 – 1500 ppm and (2) 2500 – 4000 ppm. While the first salinity range reflected the salinity of an estuary, the latter represented that of swimming pool. Under laboratory-controlled settings, the fingerprints were left aged in water for up to 15 days while routine measurement of the physicochemical parameters of the water (i.e. pH, temperature, and salinity) were made *in situ*, daily.

For every 5 days interval, the left and right equal halves of fingerprints immersed in both conditions were visualised using the SPR and NBR, respectively. About 2 mins incubation time (at room temperature) was allowed for the NBR-treated fingerprints prior to gently rinsing them under a running tap water. Subsequently, the SPR- and NBR-visualised fingerprints were left to air-dry before preserving them *via* high resolution photography. As suggested by the International Fingerprint Research Group (IFRG) [13], the quality of visualised fingerprints was evaluated using the University of Canberra (UC) comparative scale (Table 1).

Characterisation of NBR using ATR-FTIR and FESEM

For ATR-FTIR analysis, a small amount of F-MWNCTs and lyophilised NBR powders were separately placed on the acetone-cleaned ATR diamond and subsequently locked with a high-pressure clamp. The powder samples were individually scanned from $650 - 4000$ cm^{-1} with a spectral resolution of 8 cm^{-1} for over 8 times. On the other hand, FESEM analysis was done at an accelerating voltage of 5 kV and an electric current 10 μA. While the F-MWCNTs powder was placed directly on a double-sided carbon tape on a FESEM stab, a thin film of platinum was sputter-coated onto the NBR-visualised fingerprints deposited on a glass cover slip for avoiding unwanted charging under the electron beams. Both samples were then separately analysed.

Table 1 The UC comparative scale used to assess the performance of two detection methods (A and B)* applied to split fingerprints

Score	Definition
+2	Half-impression developed by method A exhibits far greater ridge detail and/or contrast than the corresponding half-impression developed by method B.
+1	Half-impression developed by method A exhibits slightly greater ridge detail and/or contrast than the corresponding half-impression developed by method B.
0	No significant difference between the corresponding half-impressions.
-1	Half-impression developed by method B exhibits slightly greater ridge detail and/or contrast than the corresponding half-impression developed by method A.
-2	Half-impression developed by method B exhibits far greater ridge detail and//or contrast than the corresponding half-impression developed by method A.

*Method A was for SPR, while method B was for NBR

In silico characterisation of NBR with that of lipid constituents of fingerprints

Molecular docking simulation

Both AutoDock 4.2 [14] and AutoDock Vina [15] software were used for *in silico* simulation of the best fit orientation of the NBR (CRL being the receptor) with selected fatty acids found in fingerprints (i.e. palmitic and oleic acids) (ligands). Databases such as Protein Data Bank and PubChem were utilised for obtaining the 3-dimensional structures of CRL (1TRH) and the aforementioned fatty acids. Respectively, the Kollman and Gasteigher chargers as well as hydrogen atoms were added to both structures prior molecular docking analysis using AutoDock 4.2 software. Taking into account the position of the catalytic triad of CRL (Ser-209, Glu-341 and His-449), the search space (grid box) was set to $18 \times 18 \times 18$ grid points with centre points of 62.22 (x), 49.82 (y) and -16.57 (z) at 1.0 Å grid spacing. For estimating the best fit orientation of CRL-fatty acid complexes with the lowest binding energy, AutoDock Vina software was used and the resultant structures were viewed with PyMOL software [16].

Molecular dynamics simulation

To account for the flexibility and genuineness of the CRL-fatty acids interactions, molecular dynamics simulation was performed. Using Avogadro software [17], the relevant hydrogen atoms were added to the docked ligands and its respective topologies files were generated with the aid of Automated Topology Builder server [18]. Subsequently, the itp and original geometry pdb files (united-atom format) were used for molecular dynamics simulation.

Running on Linux operating system, the CRL-fatty acid complexes were simulated using GROMACS software (version 2018.6) with Gromos 54a7 force field [19]. For each CRL-fatty acid complex centred in the virtual 1.0 Å cubic simulation box, approximately 22091SPC/E water molecules were used to solvate the system prior to neutralising 17 solvent ions with 17 sodium ions. Next, the system was minimised for ~399 steps following that of steepest descents method and leap-frog algorithm and equilibrated at 300 K. In triplicates, each of the CRL-fatty acid complex were allowed to simulate for 100 ns (100,000 ps) with integration time steps of 2 fs. The resultant simulation trajectories were then analysed using GROMACS tools *via* gmx rms function.

## RESULTS AND DISCUSSIONS

Characterisation of NBR using ATR-FTIR

Figure 1 illustrates the ATR-FTIR spectra of (a) F-MWCNTs and (b) CRL-MWCNTs (NBR) respectively. The broad O-H stretching appeared in both spectra (3643.60 cm^{-1} and 3615.03 cm^{-1}) were due to the atmospheric moisture that presumably bounded tightly to the sidewalls of F-MWCNT. Additionally, oxidation reaction happened during the purification of raw MWCNTs [20] may had contributed to the observed broad O-H stretching too. Acid functionalisation of purified MWCNTs using a mixture of concentrated HNO_3 and H_2SO_4 resulted in the formation of C=O stretching (1642.80 cm^{-1}) and O-H stretching (3026.06 cm^{-1}) that corresponded with the existence of carboxylic groups [21]. Observably, a number of medium intensities, reduced and expanded vibration bands ranged between 1000-1300 cm^{-1} belonging to the carboxylate groups, thereby signifying successful immobilisation of CRL onto the F-MWCNTs. In addition, peak observed at 1640.20 cm^{-1} was characteristic of C=O stretching of amide from the polypeptide chains of CRL. This too, further supported the successful immobilisation of CRL onto the functionalised nanotubes. Altogether, the findings observed here were in accordance with the previously reported studies [10,22]. The observed wavelengths and its respective functional groups are summarized in Table 2.

Characterisation of NBR-visualised fingerprint using FESEM

The topographic details of (a) powder F-MWCNTs and (b) NBR on a fingerprint were shown in Figure 2. Observably, the overall range diameter of the functionalised nanotubes was increased from 13.0 – 15.4 nm to 21.9 – 26.8 nm. The increased diameter further supported the fact that the CRL was indeed physically adsorbed onto the F-MWCNTs; a commonly reported observation [8,10,21]. Similarly, the observed 'rough surfaces' seen in Figure 2 (b) illustrated that the

CRL was encasing the entire surface of the functionalised nanotubes, a phenomenon described as the 'evenness of enzyme 'coating'' [23]. The thickening and rough surface of the NBR was due to the fact that CRL naturally tended to form bimolecular aggregates on functionalised surfaces [24,25]. Additionally, the results showed here also corroborated the ATR-FTIR findings discussed previously.
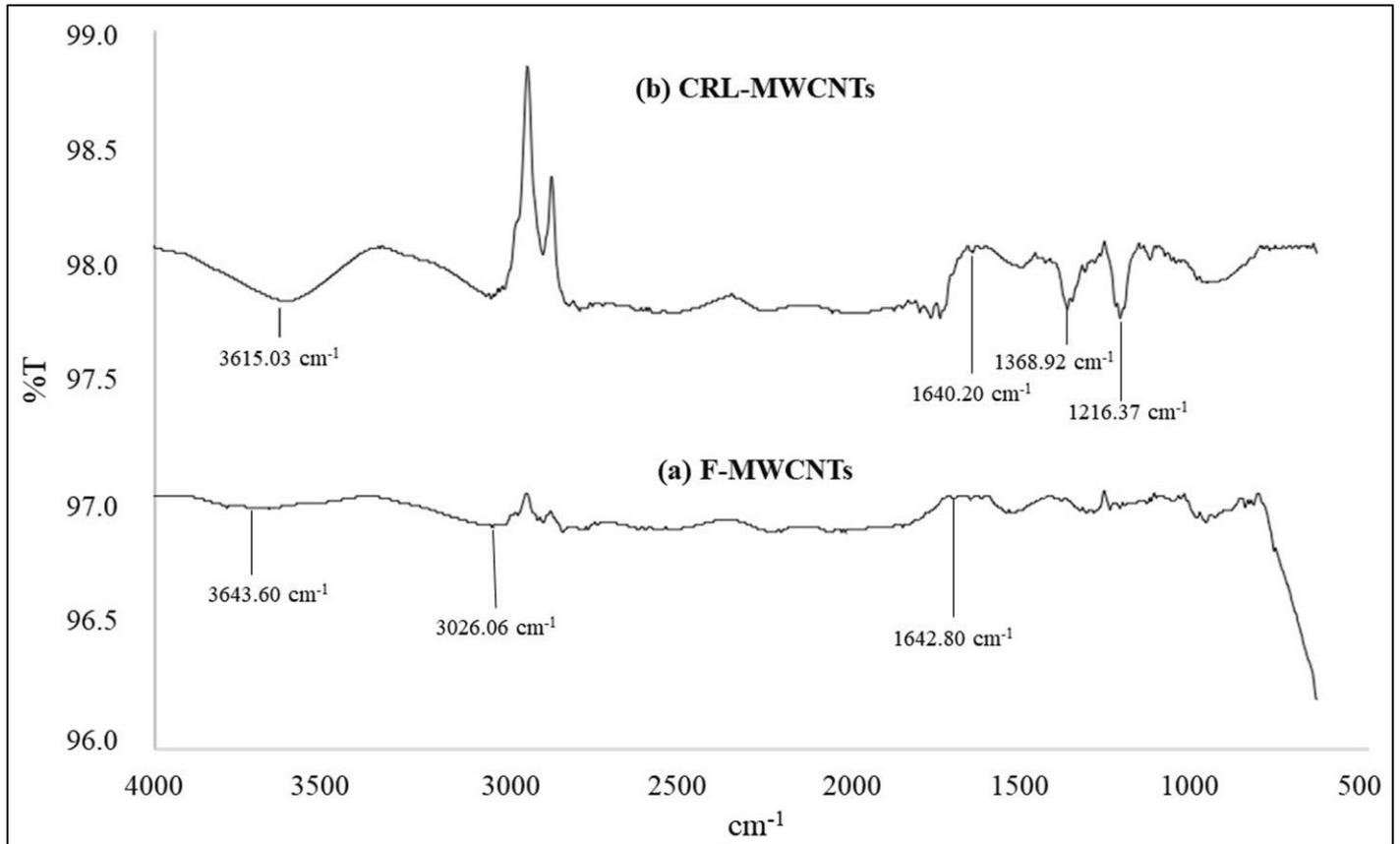
Figure 1 The ATR-FTIR spectra of (a) F-MWCNTs and (b) CRL-MWCNTs (NBR)

Table 2 The observed wavelengths and its respective functional groups in the ATR-FTIR spectra of F-MWCNTs and CRL-MWCNTs (NBR)

Wavelength (cm^{-1})	Functional groups
3026.06, 3615.03, 3643.60	O-H stretching
1640.20, 1642.80	C=O stretching
1000 – 1300	carboxylate
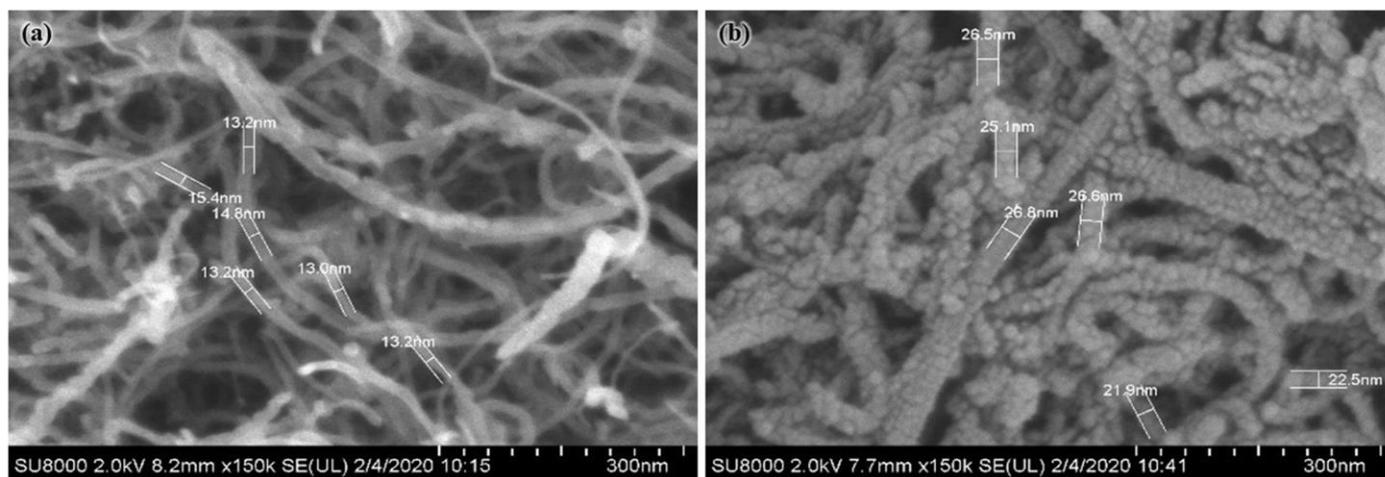
Figure 2 FESEM photographs of (a) powder F-MWCNTs and (b) CRL-MWCNTs (NBR) on a fingerprint under 150,000x magnification

Analysis of molecular docking simulation

Molecular docking simulation was conducted between the CRL and two fatty acids found in the wet fingerprint residues that were reported by Azman et al. [10], which were palmitic and oleic acids. In this study, the two fatty acids were separately docked into the active site of CRL consisted of catalytic triad *viz.* Ser-209, Glu-341, and His-449. Results from AutoDock Vina revealed that oleic acid yielded the lowest binding free energy (-5.4 kcal/mole), followed by palmitic acid (-5.1 kcal/mole). The binding free energy value was associated with the interaction stability between the ligand (fatty acids) and the protein (CRL) [26]. The lower the binding free energy, the lesser the energy required for ligand to interact with protein, therefore the more stable CRL-fatty acid complex is. Additionally, the results obtained here also showed that oleic acid would bind tighter to CRL than palmitic acids, despite the fact that CRL has been reported to have a higher preference towards short chain unsaturated fatty acids [27]. However, a recent study had found out that the CRL was more efficient in catalysing long-chain unsaturated fatty acids (oleic acid) compared to medium-chain saturated fatty acids (palmitic acid) [28]. Nevertheless, this present study would like to emphasize that *in silico* investigation was done to demonstrate the CRL binding capability and subsequently corroborating the successful visualisation of wet latent fingerprints following the use of NBR, rather than its ability to hydrolyse the lipids.

Results showed that hydrogen bonds were formed between the Ser-209 and respective fatty acids in the simulated complexes. The slightly longer distance between Ser-209 and palmitic acids (2.2 Å) when compared to oleic acids (2.1 Å) (Figure 3) corresponds to the fact that the latter binds more strongly to CRL (lower binding free energy). Regardless, both of the calculated distances of the CRL-fatty acid complexes fell within the stipulated range limit of intermolecular hydrogen bonding (cut-off distance beyond 2.5 Å) [29], substantiating the feasibility of the NBR to visualise fingerprints on wet, non-porous substrates immersed in saline water.

Analysis of molecular dynamics simulation: Root mean square deviations (RMSDs)

MD simulations were performed in triplicates for 100 ns to verify the predicted modes of binding between CRL and the two fatty acids as illustrated in Figure 4. Results showed that CRL-oleic acid complex reached equilibrium around 40 ns of simulation, followed by CRL-palmitic acid complex after 70 ns. This finding indicated that CRL had a shorter duration to form a stable complex with oleic acid compared to the CRL-palmitic acid complex. It is also important to note here that both complexes fluctuated nominally throughout the individual simulations with a small variation of 0.15-0.33 nm, which implied that both complexes had achieved stability and demonstrated good quality of binding modes. More importantly, the findings obtained here further supported the sensitivity of the NBR in tracing the lipid constituents of fingerprints aged in saline water.
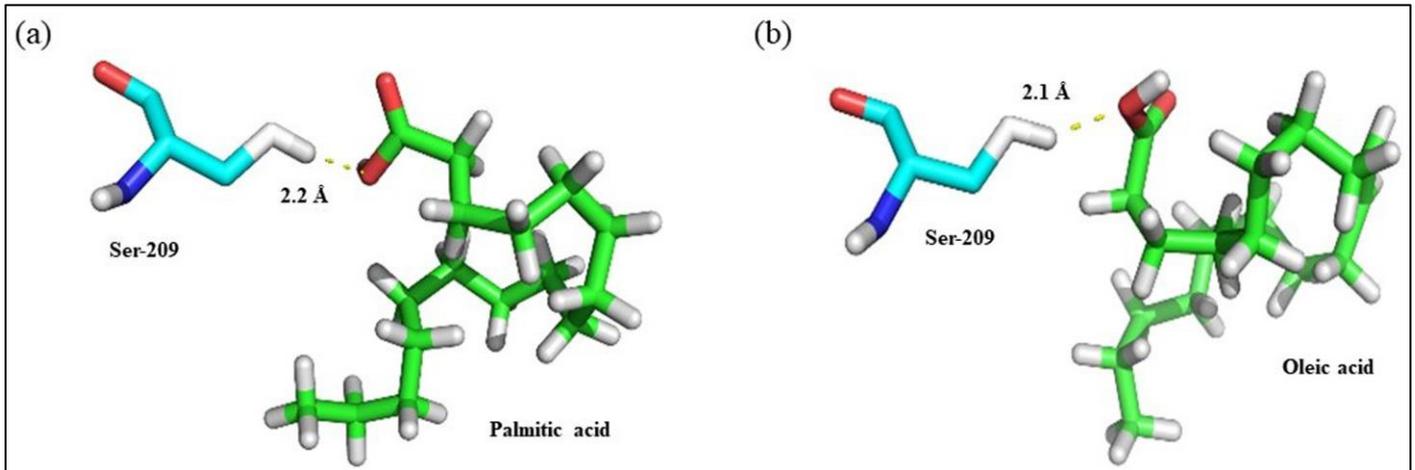
Figure 3 Formations of hydrogen bond in between Ser-209 of CRL with (a) palmitic acid and (b) oleic acid
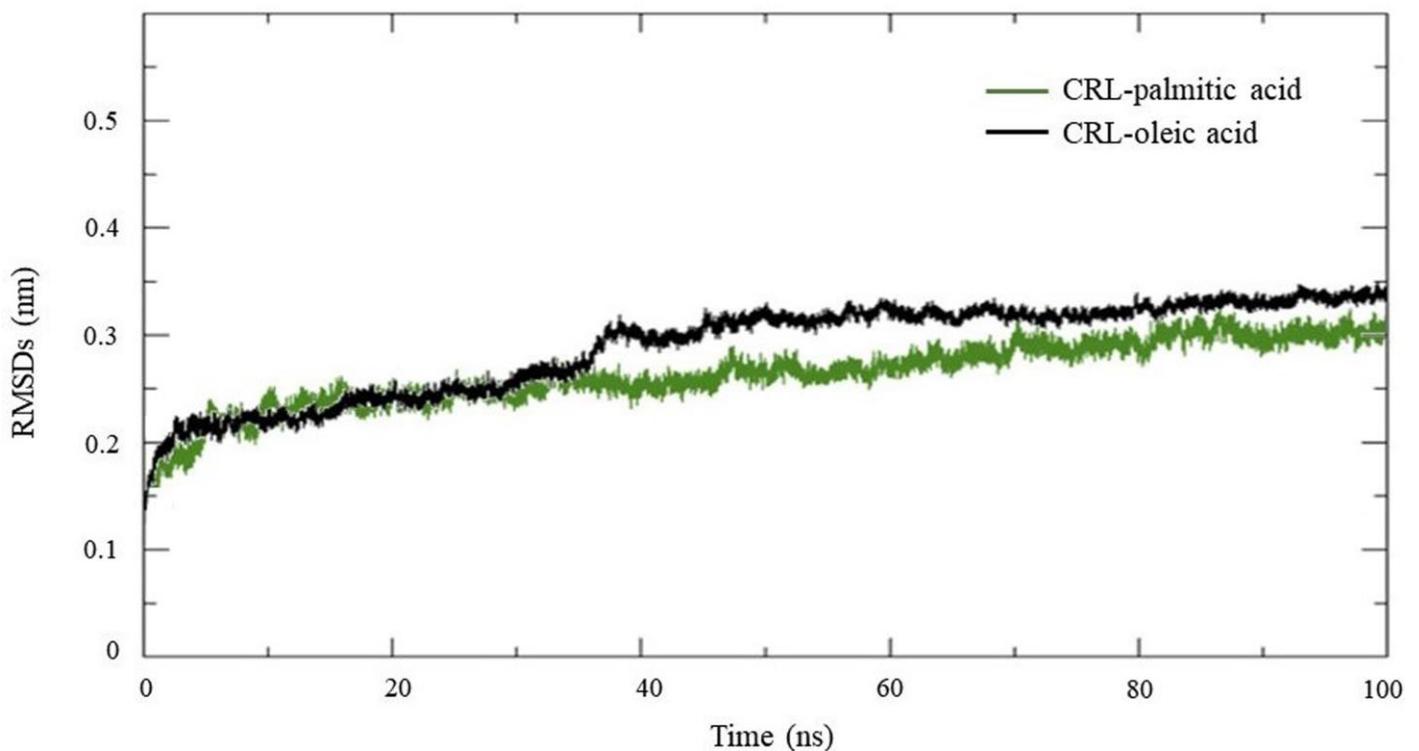
Figure 4 The average RMSDs for CRL-palmitic acid and CRL-oleic acid

Table 3 The routinely measured physicochemical parameters of the stagnant tap water in both conditions throughout the whole observation period
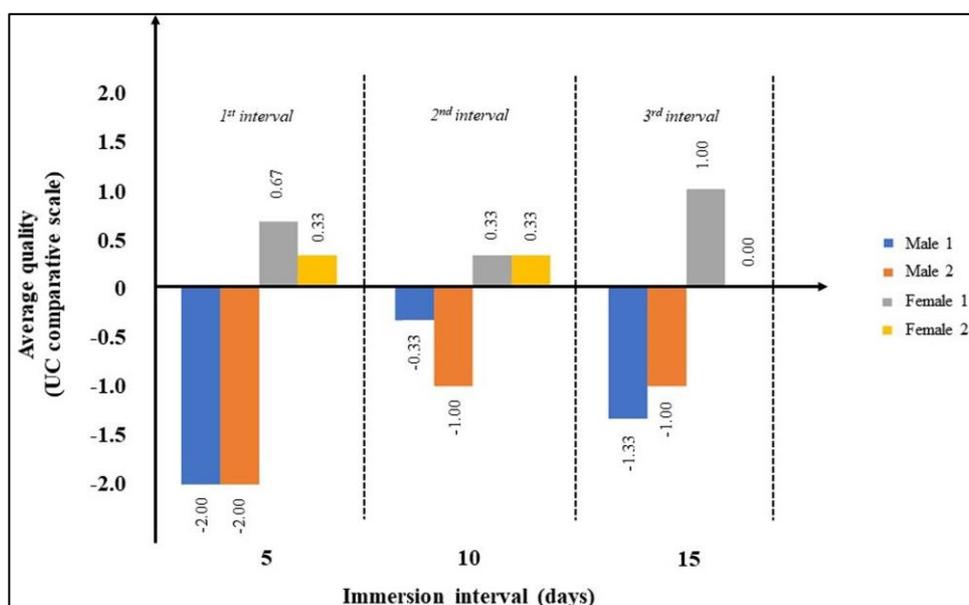
Water condition	Estuary-like	Swimming pool-like
pH	7.09 – 7.15	7.30 – 7.37
Temperature (°C)	26.0 – 29.0	26.0 – 28.5 °C
Salinity (ppm)	800 - 1000	2600 - 3000

## Visualisation of wet latent fingerprints using NBR and SPR

The physicochemical parameters of both water conditions were tabulated in Table 3. Noticeably, the pH of the water remained neutral for both estuary- (pH: 7.09 – 7.15) and swimming pool-like (pH: 7.30 – 7.37) conditions, consistent with the pH of natural estuary (range of pH: 7.00 – 7.50) [30] and swimming pool (range of pH: 7.20 – 7.80) [31]. Because the study was conducted under laboratory-controlled settings, the recorded temperature here was as similar as that of room temperature (ranged between 26.0 – 29.0 °C for both water conditions). As for the water salinity level, routine measurements were made throughout the observation period to ensure that the water salinity remained within the stipulated range of salinity investigated in this present study (i.e. estuary-like: 800 – 1500 ppm and swimming pool-like: 2500 – 4000 ppm).

Figures 5 and 6 represent the average quality of visualised fingerprints immersed in estuary- and swimming pool-like salinity stagnant tap waters for up to 15 days. Expectedly, the average quality of visualised fingerprints from both of the male donors immersed in estuary- and swimming pool-like stagnant tap water for 15 days were slightly superior to the female donors. Such an observation was corroborated by the fact that males secreted more sebaceous constituents than females, albeit it was reported to be statistically insignificant [32]. Because of the abundant amount of deposited lipids, the average quality of NBR-visualised fingerprints was greatly improved from UC comparative scale of 0.00 to -2.00. Interestingly, overall average quality of visualised fingerprints did not arise to above the scale of 1, thereby implying that the NBR performed consistently better than SPR throughout the whole 15 days of observation, both in estuary- and swimming pool-like conditions. It is pertinent to indicate here that scale of -2 would signify that NBR performed much better than SPR, while 0 means there is no significant difference observed between the two visualisation methods (Table 1). Therefore, it can be construed that the UC comparative scale of 0 given here indicated that the performance of NBR was comparable to the routinely used SPR; failed to develop satisfactory ridge details for forensic fingerprint identification purposes. While the commonly reported heavy background staining of SPR was also observed in this present study [10], such an observation was not seen for NBR-visualised fingerprints. This was because unlike SPR, the NBR specifically traced the minute amount of available lipids, thereby justifying almost no/less observed background staining. This finding too, was in concordance with the previously reported studies [8,10]. The representative photograph of SPR- and NBR-visualised split fingerprint is presented in Figure 7.

Figure 5 The average quality of visualised fingerprints immersed in estuary-like salinity stagnant tap water for up to 15 days
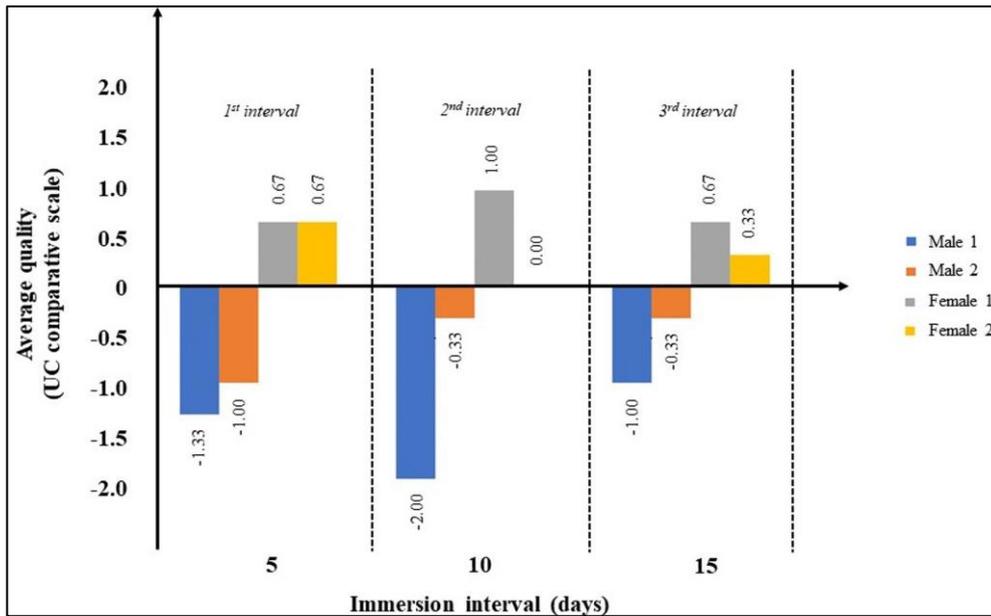
Figure 6 The average quality of visualised fingerprints immersed in swimming pool-like salinity stagnant tap water for up to 15 days
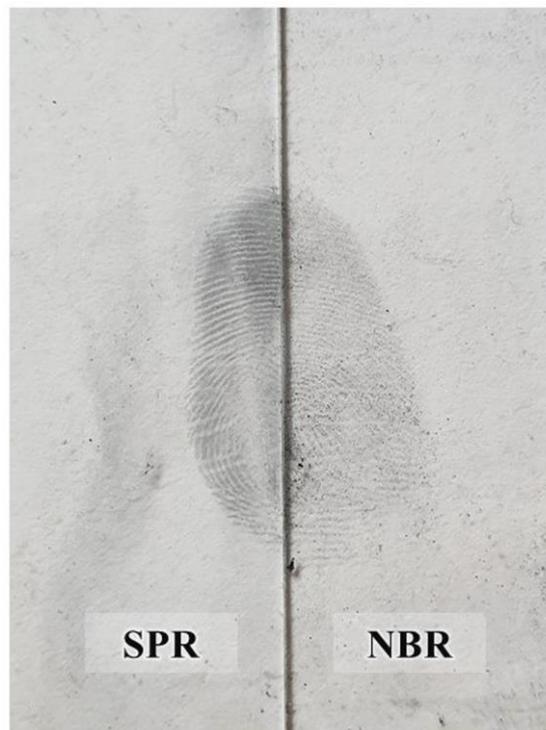
Figure 7 The representative photograph of SPR- and NBR-visualised split fingerprint on water-immersed glass slides

In addition, it was observed that longer period of immersion and higher water salinity had accelerated the rate of fingerprint degradation in both estuary- and swimming pool-like (average quality: -2.00 – 0.00), with an exception on the 2nd immersion interval (10 days) (Figures 5 and 6). Noticeably for Male 1 and Female 1 donors in estuary-like condition, the performance of NBR was slightly reduced before showing an increase on the following observation interval (Male 1: from -0.33 to -1.33 and Female 1: 0.33 to 1.00) (Figure 5). Similarly, for swimming pool-like condition on the 10th day of observation, both aforesaid donors had peculiar trend of 'decreasing-increasing' relative performance of both visualisation methods (Figure 6). While the UC comparative scale for Male 1 for the last two observation intervals was -2.00 to -1.00, Female 1 was given a scale of 1.00 to 0.67 for the swimming pool-like condition. Nonetheless, the findings obtained here substantiate the fact that the newly developed NBR was able to visualise latent fingerprints on wet, non-porous substrates immersed even in destructive (i.e. different levels of water salinity) conditions.

CONCLUSION

This study had successfully characterised the immobilisation of CRL onto F-MWCNTs using ATR-FTIR and FESEM. The bioinformatics analysis further confirmed the presence of hydrogen bonds between the NBR and lipid-soluble constituents of wet fingerprints. Both NBR and SPR were able to visualise split groomed fingerprints immersed in water with salinity of estuary- and swimming pool-like for up to 15 days of immersion. Results revealed that the NBR performed better in visualising fingerprints compared to the commercially available SPR (UC comparative scale of -2) due to the high specificity and selectivity of NBR towards the lipid-soluble constituents of fingerprints. Considering that NBR is made up of non-toxic chemical like CRL and the fact that its performance remarkably surpassed that of the routinely used SPR, therefore its practical utilisation as the safer and greener alternative reagent in visualising fingerprints on wet, non-porous substrates appears to be supported.

Conflict of Interest

Authors declare none.

Authors' contribution

CWT conducted the scientific experiments, analysis, and interpretation of the data. NAM and ARA were responsible for supervision, conceptualisation, and critical revision of the paper. NWM and NA were responsible for the manuscript preparation. All the authors have read and gave approval for submission.

REFERENCES

1. Subhani Z, Daniel B, Frascione N. DNA profiles from fingerprint lifts - Enhancing the evidential value of fingermarks through successful DNA typing. J Forensic Sci. 2019; 64(1): 201-206.
2. Kasper SP. The processes. Latent Print Processing Guide, 1st edn. Elsevier Inc., San Diego, California. 2016: 49-167.
3. Dhall JK, Kapoor AK. Development of latent prints exposed to destructive crime scene conditions using wet powder suspensions. Egypt J Forensic Sci. 2016; 6(4): 396-404.
4. Madkour S, Abeer S, El Dine FB, Elwakeel Y, AbdAllah N. Development of latent fingerprints on non-porous surfaces recovered from fresh and sea water. Egypt J Forensic Sci. 2017; 7(1): 3.
5. Houck MM, Siegel JA. Friction ridge examination. Fundamentals of Forensic Science, 3rd edn. Elsevier Ltd, San Diego, California. 2015: 493-518.
6. Bumbrah GS. Small particle reagent (SPR) method for detection of latent fingermarks: A review. Egypt J Forensic Sci. 2016; 6(4): 328-332.

7. International Agency for Research on Cancer (2010) IARC monographs on the evaluation of carcinogenic risks to humans. International Agency for Research on Cancer, Lyon, France

8. Azman AR, Mahat NA, Abdul Wahab R, Abdul Razak FI, Hamzah HH. Novel safranin-tinted *Candida rugosa* lipase nanoconjugates reagent for visualizing latent fingerprints on stainless steel knives immersed in a natural outdoor pond. Int J Mol Sci. 2018; 19(6): 1576.

9. Azman AR, Zulkifli NS, Mahat NA, Ahmad WA, Hamzah HH, Abdul Wahab R. Visualisation of latent fingerprints on non-porous object immersed in stagnant tap water using safranin-tinted *Candida rugosa* lipase reagent. Malay J Fundamental App Sci. 2019; 15(6): 781-783.

10. Azman AR, Mahat NA, Wahab RA, Ahmad WA, Huri MAM, Hamid AAA, Adamu A, Saat GAM. Characterisation and computational analysis of a novel lipase nanobio-based reagent for visualising latent fingerprints on water-immersed glass slides. Process Biochem. 2020; 96: 102-112.

11. Wahab RA, Puspanadan JK, Mahat NA, Azman AR, Ismail D. Potassium triiodide enhanced multi-walled carbon nanotubes supported lipase for expediting a greener forensic visualization of wetted fingerprints. Chemical Papers. 2020; 1-12.

12. Bruce E. Rittmann, McCarty PL. Moving toward sustainability. Environmental biotechnology: Principles and applications, 2nd edn. McGraw-Hill Education, New York, USA. 2020: 1-8.

13. International Fingerprint Research Group. Guidelines for the assessment of fingermark detection techniques. J Forensic Ident. 2014; 64(2): 174 - 200.

14. Morris GM, Huey R, Lindstrom W, Sanner MF, Belew RK, Goodsell DS, Olson AJ. AutoDock4 and AutoDockTools4: Automated docking with selective receptor flexibility. J Comput Chem. 2009; 30(16): 2785-2791.

15. Trott O, Olson AJ. AutoDock Vina: improving the speed and accuracy of docking with a new scoring function, efficient optimization, and multithreading. J Comput Chem. 2010; 31(2): 455-461.

16. Schrödinger L. The PyMOL Molecular Graphics System. 2015.

17. Hanwell MD, Curtis DE, Lonie DC, Vandermeersch T, Zurek E, Hutchison GR. Avogadro: An advanced semantic chemical editor, visualization, and analysis platform. J Cheminformatics. 2012; 4(1): 17.

18. Malde AK, Zuo L, Breeze M, Stroet M, Poger D, Nair PC, Oostenbrink C, Mark AE. An automated force field topology builder (ATB) and repository: Version 1.0. J Chem Theory Comput. 2011; 7(12): 4026-4037.

19. Van Der Spoel D, Lindahl E, Hess B, Groenhof G, Mark AE, Berendsen HJ. GROMACS: fast, flexible, and free. J Comput Chem. 2005; 26(16): 1701-1718.

20. Mohamad NR, Buang NA, Mahat NA, Lok YY, Huyop F, Aboul-Enein HY, Wahab RA. A facile enzymatic synthesis of geranyl propionate by physically adsorbed *Candida rugosa* lipase onto multi-walled carbon nanotubes. Enzyme Microb Tech. 2015; 72: 49-55.

21. Che Marzuki NH, Mahat NA, Huyop F, Aboul-Enein HY, Abdul Wahab R. Sustainable production of the emulsifier methyl oleate by *Candida rugosa* lipase nanoconjugates. Food Bioprod Process. 2015; 96: 211-220.

22. Che Marzuki NH, Huyop F, Aboul-Enein HY, Mahat NA, Abdul Wahab R. Modelling and optimization of *Candida rugosa* nanobioconjugates catalysed synthesis of methyl oleate by response surface methodology. Biotechnol Biotechnol Equip. 2015; 29(6): 1113-1127.

23. Shah S, Solanki K, Gupta MN. Enhancement of lipase activity in non-aqueous media upon immobilization on multi-walled carbon nanotubes. Chem Cent J. 2007; 1: 30.

24. Fernandez-Lorente G, Palomo JM, Fuentes M, Mateo C, Guisan JM, Fernandez-Lafuente R. Self-assembly of *Pseudomonas fluorescens* lipase into bimolecular aggregates dramatically affects functional properties. Biotechnol Bioeng. 2003; 82(2): 232-237.

25. Palomo JM, Ortiz C, Fernández-Lorente G, Fuentes M, Guisán JM, Fernández-Lafuente R. Lipase–lipase interactions as a new tool to immobilize and modulate the lipase properties. Enzyme Microb Tech. 2005; 36(4): 447-454.

26. Earlia N, Muslem, Suhendra R, Amin M, Prakoeswa CRS, Khairan, Idroes R. GC/MS analysis of fatty acids on pliek u oil and its pharmacological study by molecular docking to filaggrin as a drug candidate in atopic dermatitis treatment. The Scientific World Journal. 2019; 2019: 8605743-8605743.

27. Schmitt J, Brocca S, Schmid RD, Pleiss J. Blocking the tunnel: Engineering of *Candida rugosa* lipase mutants with short chain length specificity. Protein Eng. 2002; 15(7): 595-601.

28. Sri Kaja B, Lumor S, Besong S, Taylor B, Ozbay G. Investigating enzyme activity of immobilized *Candida rugosa* lipase. Journal of Food Quality. 2018.

29. Pokhrel R, Bhattarai N, Baral P, Gerstman BS, Park J, Handfield M, Chapagain P. Molecular mechanisms of pore formation and membrane disruption by the antimicrobial lantibiotic peptide mutacin 1140. Phys Chem Chem Phys. 2019; 21: 12530-12539.

30. Ronald L. Ohrel J, Register KM. Volunteer Estruary Monitoring: A Methods Manual. The Ocean Conservancy, Washington, DC. 2006.

31. Clark JR. Guide to Swimming Pool Maintenance. PWPH Publications. 2012.

32. Croxton RS, Baron MG, Butler D, Kent T, Sears VG. Variation in amino acid and lipid composition of latent fingerprints. Forensic Sci Int. 2010; 199(1-3): 93-102.